Title: Microfluidic Manufacture of Solid Lipid Nanoparticles: A case study on tristearin-based systems.

Authors: Giulia Anderluzzi and Yvonne Perrie

Strathclyde Institute of Pharmacy and Biomedical Sciences, University of Strathclyde, Glasgow G4 0RE

Key Words: solid lipid nanoparticles, Microfluidics, protein delivery, manufacture.

Corresponding author:

Professor Yvonne Perrie
Strathclyde Institute of Pharmacy and Biomedical Sciences,
161 Cathedral St,
University of Strathclyde,
Glasgow, G4 0RE
Scotland.
yvonne.perrie@strath.ac.uk

ABSTRACT

Background: Solid lipid nanoparticles are lipid-based carriers and that can be used for a range of drugs and biomolecules. However, most production methods currently used do not offer easy translation from laboratory preparation to scale-independent production.

Objectives: Within this study, we have investigated the use of microfluidics to produce solid lipid nanoparticles and investigated their protein loading capability. In the development of the process, we have investigated and identified the critical process parameters that impact on the production of the solid lipid nanoparticles.

Method: Solid lipid nanoparticles based on Tristearin and 1,2-Distearoyl-phosphatidylethanolamine-methyl-polyethyleneglycol conjugate-2000 were formulated using on the Nanoasemblr® Benchtop system from Precision Nanosystems and the flow rate ratio, total flow rate and initial protein concentration were investigated as process parameters and the particle size, PDI, zeta potential, drug loading and drug release was quantified.

Results: Our results demonstrate the suitability of microfluidics as a valid poduction method for solid lipid nanoparticles containing protein production. In terms of key process parameters to consider, both the solvent/aqueous ratio (FRR) and total flow rate were shown to have a notable impact on particle size. However, protein loading capacity was similar across all flow rates tested.

Conclusion: Within this study we outline a rapid and easy to adopt protocol for the scale-independent production of solid lipid nanoparticles. This process can support the rapid translation of production methods from bench to clinic.

1. Introduction

Microfluidics technology is based on controlled manipulation and mixing of fluids in the microliter to picolitre range. Since its first application in the 1980s [1], microfluidics has emerged as a lab-on-a-chip based technology for process development [2-3], to automate laboratory procedures in the fields of pharmaceutical industry and biotechnology [4] and to produce nanomedicines [5-9]. Indeed, the rise in the number of publications on PubMed referencing microfluidic* is shown in Figure 1 and can be seen to have grown to approximately 2500 since 1988. In general, microfluidics involves the controlled mixing of fluids, with fluid mixing being dictated by the design of the microfluidic cartridge (with numerous formats and mixing-steps having been investigated) and the process parameters adopted (including the flow rate through the cartridge and the mixing ratios employed during the process). In terms of a mixing process, microfluidics offers a range of advantages including scalable working volumes from very low volumes to high-throughput, short reaction times, reduced cost, controlled mixing and enhanced parameter control combined with process automation [10-13]. Due to these advantages, microfluidics has been used to produce a range of nanoparticle systems including lipid nanoparticles, liposomes, polymeric nanoparticles and solid lipid nanoparticles with some examples outlined in Table 1. By using microfluidics to rapidly mix liquids of different polarities, the nanoprecipitation of dissolved molecules can be promoted and uniform nanoparticle suspensions produced. [40] As shown in Table 1, the majority of the investigations looking at manufacturing with microfluidics has focused on the production of liposomes with less consideration given to solid lipid nanoparticles (SLNs). This may be due to solid lipid nanoparticles being less widely studied as potential delivery systems;

a PubMed search identifying only around 200 publications associated with these systems (Figure 1). However, as delivery systems, solid lipid nanoparticles can offer a range of advantages including enhanced stability compared to other lipid-based formulations, sustained release and increased tolerability compared to polymeric systems [41-43]. However, lipid all nanoparticles, large scale production can be a challenge. In terms of their application, SLNs are more commonly explored as solubilising agents for the delivery of poorly soluble drugs due to the hydrophobic nature of the particles matrix. However, they have also been investigated for the delivery of nucleic acids, proteins, antigens, or in food industry as carriers for bioactive compounds or to protect biomolecules against degradation[44-46]. Within our research, we are considering a range of delivery systems for their potential as novel adjuvants and studies have demonstrated that SLNs have an adjuvant activity. In general, the adjuvant effect of SLNs is related to their ability to protect sub-unit antigens from rapid degradation in vivo, and to promote delivery and targeting of antigen presenting cells [47]. With regard to their activity, particle size is a consideration with some studies suggesting that SLNs with a diameter of more than 100 nm exhibited a stronger adjuvant activity [48-49]. Furthermore, SLNs in association with interleukin-2 have been shown to increase antibody titre, spleenocyte proliferation, and secretion of interferon-gamma and interleukin 4 cytokines. [50]

In terms of manufacturing processes, high-pressure homogenization [51] and microemulsion-based techniques [52-54] are the most used methods in the preparation of SLNs. Yet, these methods have limitations including ease of scalability and poor drug loading capacity. Therefore, given the potential of microfluidics to produce nanoparticles, herein we consideration the application of microfluidics for rapid and scale-independent manufacture of solid lipid nanoparticles. To achieve this, we have investigated the process parameters

involved in their microfluidic production and consider the loading of protein within these systems.

2. Materials and Methods

2.1 Materials

Tristearin (Grade II-S, ≥90%) and trifluoracetic acid (TFA) were obtained from Sigma-Aldrich Company ltd, Poole, UK. 1,2-Distearoyl-phosphatidylethanolamine-methyl-polyethyleneglycol conjugate-2000 (DSPE-mPEG-2000) was obtained from Lipoid GmbH (Ludwigshafen Germany). Ethanol were obtained from Fisher 141 Scientific UK, Loughborough, UK. TRIS Ultra-Pure was obtained from ICN 142 Biomedicals, Inc., Aurora, Ohio. Phosphate-buffered saline (PBS) and Albumin from chicken egg (OVA), were obtained from Sigma-Aldrich Company ltd, Poole, UK. Sephadex G-75 size exclusion columns were obtained from GE Healthcare Life Science -Little Chalfont-Buckinghamshire, UK.

2.2 Preparation of solid lipid particles using Nanoassemblr platform

Solid lipid nanoparticles formulations using the micromixer were performed on a benchtop NanoAssemblr™ instrument (NanoAssemblr™, Precision Nano- Systems Inc.). The two inlet streams comprised lipids dissolved in ethanol and aqueous buffer (Tris, 10 mM, pH 7.4), syringe pumps allowed for controlling the flow rates and the flow ratios between the two inlet streams. Solid lipid nanoparticles were prepared with the NanoAssemblr™; 1.3 mg of Tristearin 0.25 mg of mPEG-DSPE were dissolved in 1 mL of ethanol (70°C) and OVA (when added) was dissolved in 1 mL TRIS buffer pH 7.4 10 mM. Both solutions mixed via microfluidics and particles were collected in a 15-mL falcon tube. The total flow rate (TFR) was varied

between 5 and 20 mL/and the aqueous/solvent ratio (FRR) was varied between 1:1, 3:1 and 5:1.

2.3 Solvent purification methods

To consider solvent purification methods, residual solvent levels were quantified after tangential Flow Filtration (TFF – KR2i TFF System® – Filtration speed 27 mL/min, washing volume 20 mL), dialysis (1-hour, membrane cut off 14 000 KDa) and spin column (3 mL elution buffer volume). Residual solvent was detected using gas chromatography (GC-MS, Agilent Technologies) adding 1% 2-propanol (IPA) as internal standard; peaks area was normalised by IPA peak area and related to solvent concentration through a calibration curve with a linearity of R^2 = 0.9502. All measurements were within the level of detection and level of quantification.

2.4 Lipid recovery quantification after purification

Lipid recovery after dialysis, TFF and spin column was performed by adding 1,1'-Dioctadecyl-3,3,3',3'-Tetramethylindocarbocyanine Perchlorate (DilC) 0.2% mol total lipid concentration solved in ethanol to lipid stocks before being loaded in the NanoAssemblr. DilC fluorescence was measured before and after TFF, dialysis and spin column (PolarStar, BMG LABTECH GmbH). Lipid quantification was achieved by referring to a calibration curve with a linearity of R^2=0.995. All measurements were within the level of detection and level of quantification.

2.5 Characterisation of SLNs

The dynamic light scattering (DLS) technique was used to report the intensity mean diameter (z-average) and the polydispersity of all solid lipid nanoparticles formulations (Malvern Zetasizer Nano-ZS (Malvern Instruments, Worcs., UK). Particles size and polydispersity

analysis was carried out at 25 °C in Tris buffer (10 mM, pH 7.4). Liposome zeta potential was measured in Tris buffer (10 mM, pH 7.4) using the Malvern Zetasizer Nano-ZS (Malvern Instruments, Worcs., UK).

2.6 Protein loading quantification.

The loading efficiency was measured using reverse phase HPLC (Agilent 1100 Series) with a mobile phase of TFA 0.1 % and methanol with 0.08% TFA with a flow rate of 2.0 mL/min, λmax of 215 nm. At these conditions the OVA retention time is 9.6 min. The particles were destroyed using a solution of IPA: TRIS 50:50 vol/vol. The solution was left at room temperature for 1 hour to achieve the complete particle dissolution. All measurements were within the level of detection and level of quantification.

2.7 In vitro release study

For the release study of 0.5 mg/mL ovalbumin from SLNs, nanoparticles were prepared using Nanoassemblr (TFR 10 mL/min, FRR 3:1) as previously described. All formulations were dialysed against 80 mL PBS pH 7.4 at 37 °C (membrane cut off 300KDa). The absorbance of aliquots from the outer buffer was analysed at different time points (0.25, 0.5, 0.75, 1, 1.5, 2, 4, 6, 8, 10, 12, 24 and 48 h) using NanoDrop 2000c UV-Vis spectrophotometer (Thermo Fisher Scientific Inc). OVA release was detected by measuring the protein absorbance at 230 nm (NanoDrop 2000c, UV-Vis Spectrophotometer).

2.8 Statistical analysis

Unless stated otherwise, the results were calculated as mean ± standard deviation (SD) from three independent studies. ANOVA followed by Tukey post hoc analysis was performed for

comparison and significance was acknowledged for p values less than 0.05. All the calculations were made using Excel (Excel Software and Systems Pvt. Ltd.).

3. Results

3.1 SLNs manufacturing by microfluidics– particles size can be in process controlled

Solid lipid nanoparticles consisting of Tristearin and PEG-DSPE were prepared using the microfluidics method and the aim of this study was to evaluate how process parameters impact on particles size and polydispersity. More precisely the percentage of organic phase was reduced from 50% to 17% and differences in particles attributes were evaluated. Figure 2A showed the effect of modifying flow rate ratio (FRRs; ratio between organic and aqueous phase) on SLNs size distribution; by enhancing the FRR from 1:1 to 3:1, the diameter was reduced from 180 ± 65 nm to 65 ± 23 nm; however further increasing the FRR to 5:1 did not significantly impact on the particle size (59 ± 17 nm; Figure 2A). Across the FRR tested the PDI remained low was between 0.2 and 0.3 (figure 2A) and the size intensity plots are shown in figure 2B. Regarding particles charge, the zeta potential values was independent from the FRR (Figure 2C); among all aqueous/solvent ratio tested, the surface charge remained slightly negative (between -17 and -20 mV) as expected, with no significant difference.

3.2 Purification process for SLNs produced by microfluidics

Given that after microfluidics samples contain organic solvent, several purification methods were investigated. Tristearin: mPEG-DSPE SLNs were prepared using microfluidics at a FRR 1:1; in these conditions the concentration of ethanol in the final sample is 50 %, thus aiming to challenge all purification systems tested. To remove solvent content from the formulations

dialysis, tangential flow filtration (TFF) or spin column purification was employed and SLN recovery and residual solvent levels compared (Figure 3). As it shown in figure 3A, by using either spin column or dialysis it was possible to collect almost 100% particle yield. Iin contrast recovery of SLNs after TFF purification was lower (72%; Figure 3A). Figure 3B also shows that all three methods tested could efficiently remove the organic solvent from the sample to below 1%, and both TFF and dialysis achieved residual ethanol levels belw 0.5 %, in line with ICH guidelines for residual ethanol levels.

3.3 Protein-loaded lipid particles production using Nanoassemblr: loading efficiency as a function of manufacture process

Using these optimised parameters, the next stage was to evaluate the suitability of microfluidics for producing SLNs containing proteins. To consider this, three different protein (OVA) concentrations were used and loading compared. To achieve this, initially the extraction process was optimised and drug loading was measured at different time points (3 min, 6 hours and 24 hours post digestion). Spin column purification was applied for both solvent and free protein removal. Figure 4A shows that subjecting the OVA-loaded SLNs to prolonged exposure to IPA: TRIS 50:50 vol/vol resulted in reduced protein loading, which may be a result of protein degradation in the IPA. Therefore, for all further studies, all formulations were subjected to no more than 30 min digestion. Figure 4A also shows the effect of initial OVA concentration on loading capacity; as expected with increasing initial OVA concentrations the SLNs can incorporate higher concentrations up to approximately 140 µg/mL when initial concentrations of 1 mg/mL OVA is used. When expressed as % loading efficiency, the maximum that can be achieved is 36% when an initial concentration of 0.1 mg/mL OVA is used (Figure 4B), and in terms of loading capacity (protein/lipid wt/wt) the

trend again shows increasing loading with increasing initial OVA concentrations with up to 11% (Figure 4C). Therefore, high protein loading can be achieved when high initial protein concentrations are used but this is at the expense of loading efficacy (Figure 4).

3.4 Influence of flow rate on particle characteristics and drug loading

To consider the impact of production speed of the SLNs, changes in TFR on protein loaded particles attributes were further investigated. The total flow rate values were varied from 5 mL/min to 20 mL/min, while the ratio between aqueous and solvent stream was maintained constant at 3:1. Figure 5A shows the effect of flow rate changes on particles size and polydispersity. Increasing the injection speed from 5 to 10 mL/min made no significant difference in particles size (between 70 and 90 nm); however, enhancing TFR values to 15 mL per min or above reduced the particle sizes to a minimum of 40 ± 4 nm without affecting samples homogeneity (around 0.25). The same trend was seen when particles zeta potential was measured (Figure 5B) with the zeta potential at TFR 5 mL/min being more variable at low (5 mL/min) TFRs, where charge was maintained slightly negative (around -30 mV). With respect to the loading efficiency, using an initial 0.5 mg/mL protein concentration, the capability was not significantly influenced by the total flow rate; however, less variability in protein loading was seen at flow rates of 10 mg/mL or more with loading of 80 - 90 µg/mL (Figure 5C).

The release profiles of OVA from SLNs produced was also investigated. To study this, particles were prepared from a FRR 3:1, TFR 10 mL/min and OVA initial concentration of 0,5mg/mL. The results show that the SLNs give a rapid release of up to 90% within the first 24 h and the release does not follow a zero-order profile. The release was also plotted as Ln cumulative percentage of drug released vs time (Figure 6B) and the data suggests the release does not

220 follow a first-order model. This finding suggested that a combination of more than one
221 kinetics might drive protein release from SLNs.

222 **4. Discussion**

223 This work demonstrates that microfluidics technology can be employed as an alternative
224 method for the rapid and scalable production of solid lipid nanoparticles containing
225 hydrophilic molecules. Although there has been extensive work on delivery for hydrophobic
226 molecules using SLNs (due to their lipid-based matrix facilitating drug incorporation) their
227 applicability as water soluble carries has received less attention. Therefore, to consider this,
228 we have investigated these systems for the delivery of water soluble proteins (ovalbumin).
229 Our studies demonstrate that protein-loaded SLNs can be manufactured with their particle
230 size being process controlled. Previous studies on microfluidics confirmed the effect of flow
231 rate ratio on particles dimensions, in agreement with what has been reported in the present
232 work. [55-57] For example, cationic 1,2-dioleoyl-3-trimethylammonium-propane (DOTAP)
233 based liposomes formed at 1:5 solvent/aqueous formulation were smaller in size (50–75 nm)
234 compared to the 1:1 solvent/aqueous formulation (175–200 nm) [5]. Furthermore, 1,2-
235 distearoyl-sn-glycero-3-phosphocholine (DSPC) and cholesterol liposomes formed at low flow
236 rate ratio (1:1) resulted to be larger in size (200 nm) with respect to their counterparts
237 formulated at higher FRRs (around 90–120 nm). [9] However, it was also seen that increasing
238 the FRR increased polydispersity; [6] a possible explanation to this phenomenon would be
239 related to the reduced particles fusion (Ostwald ripening) that occurred at higher FRR, due to
240 the lower amount of residual solvent. Thus, the formation of smaller monodisperse particles
241 in achieved. [58-59] On the other hand, at higher FRRs, a dilution of the organic phase occurred,
242 reducing the tendency of lipids to diffuse, with an effect on sample polydispersity; these

observations were confirmed by previous studies where a staggered herringbone mixer was used [6]. The higher is the FRR the lower is the lipid concentration and consequently the lower is the rate of diffusion. This phenomenon led to partly incomplete nucleation and a lower rate of particles formation. [60]

When considering the surface charge of the SLN particles, zeta potential values remained unchanged along FRRs tested (around -20mV; Figure 2B) as expected; Tristearin or glyceryl tristearate is a triglyceride derived from three units of stearic acid, without any charged group at neutral pH. [61-63] However, PEG-DSPE is a linear phospholipid, a block copolymer of a hydrophobic part (DSPE) and a hydrophilic part (PEG). [64-65] The phosphoethanolamine group is completely ionised at pH 7.4, giving the PEG a net negative charge. By adding PEG-DSPE to SLNs formulation the distearoyl tail is incorporated to the tristearin solid layer; instead, the hydrophilic PEG-phosphoethanolamine part remained on lipid surface, making particles negatively charged.[66-68] It is alsol known that the addition of PEG may help the manufacture of more homogeneous particles. [69]

In the development of manufacturing processes, production speed is important. Here we demonstrate that total flow rates of 20 mL/min can easily be adopted with no effect on the particle size or protein loading. This is in line with previous work on liposomes, where increasing the flow rate from 10 to 20 mL/min had no effect on liposome size, PDI or protein loading. [7] Within the microfluidic cartridge, even although the surface to volume ratio is relatively high (due to the reduced dimensions of the channels), the Reynolds number (Re=1 ρv/η) of liquid is quite low (around 1) [70-71]. In these conditions, the flow tends to be laminar and driven by diffusive forces, with a direct consequence on mixing process speed [72]. To overcome these issues, either the contact area or the contact time between solutions need

to be enhanced. To address this, the inner geometry of the cartage plays an important role with the serpentine shape of the microchannel doubling the mixing efficiency of conventional straight microchannel [9].

As part of production process, the residual ethanol concentration in the final product is one of the characteristics that must be considered. Ethanol is a Class 3 solvent, which is considered less toxic and a lower risk solvent compared to Class 1 and 2 solvents and within pharmaceuticals levels of 50 mg per day or less (corresponding to 5000 ppm or 0.5%) being acceptable without justification. [73-75]. For laboratory production of SLNs, three methods were considered and both TFF and dialysis can remove solvents to below the required ICH levels (Figure 3). Whilst TFF was shown to give slightly lower recovery compared to the other methods, TFF offers faster and scalable purification options. Tangential flow filtration is a technique that utilizes a porous barrier to separate molecules in solution based on size or molecular weight. Application of pressure across a known pore size column drives the separation process. Smaller constituents pass through the barrier with the solvent as filtrate while the larger solutes are retained [76]. In this technique the feed stream passes parallel to the membrane face as one portion passes through the membrane (permeate) while the remainder (retentate) is recirculated back to the feed reservoir. [77] TFF has already been demonstrated for the purification of other nanomedicines, for example, poly-vinyl alcohol (PVA) and sodium cholate were shown to be efficiently removed from monomethoxy poly (ethylene glycol) – poly (D, L-lactide-co-glycolide) (mPEG-PLGA) co-polymer nanoparticles using TFF, without altering particles properties. [78] Furthermore, tangential flow filtration was applied as purification method for Poly (d, l-lactic acid) nanoparticles from poloxamer 188; within this study the authors reported that purification of the nanoparticles from the excess

surfactant using tangential flow filtration enabled even better drying results when the different sugars were studied. [79]

Considering protein loading within solid lipid nanoparticles, drug loading via microfluidics is a passive mechanism, where a simultaneous dispersion of drug and lipids in the aqueous phase occurs and microfluidics can promote higher encapsulation efficiency compared to conventional techniques. Herein, we achieved high protein (OVA) loading even at lower OVA concentrations (around 40% LE at 0.1 mg/mL initial [OVA]) (Figure 4 and 5). This is higher than commonly reported for SLNs manufactured by other methods. For example, it has been seen that egg lecithin and stearic acid based SLNs made through warm microemulsion were able to encapsulate below 5% of the water soluble immunostimulant Thymopentin [80]. The same technique was applied for cyclosporine loading into SLNs made of a mixture of stearic acid and Epikuron 200®. However, the loading efficiency was not promising (just 13%) [81]. Further, supercritical fluids (e.g. CO_2) were applied to SLN manufacturing. However, many papers reported that the entrapment efficiency of small peptides – e.g. Insulin – within Tristearin based SLNs was very low (<3%) [82-83]. This improved loading via microfluidics has also been shown with other nanoparticle systems, for example, 1,2-distearoyl-sn-glycero-3-phosphocholine (DSPC) and cholesterol liposomes made by microfluidics gave 30 % protein loading (0.18 mg/mL initial OVA concentration). This is in comparison to below 5 % with lipid hydration and extrusion or sonication. [7] Furthermore, the concentration of sulforhodamine B in liposomes prepared with microfluidics was found to be unexpectedly high due to a spatial concentration enhancement induced by viscosity anisotropy in the microchannel. [84-85] Therefore, the combination of the fast production step and higher entrapment efficiency of protein demonstrates the suitability of microfluidics as effective alternative method for protein loaded solid lipid nanoparticles. In terms of release from the SLNs (Figure 6), the

majority of the protein was released within 24 h. The initial fast release of OVA maybe resulting from OVA associated at the surface layer of the solid lipid nanoparticles [86] and the PEG coating on SLNs surface could accelerate the release of proteins or drugs from lipid matrix. It has been seen [83] that PEGylated particles showed a faster protein release with an initial burst, probably due to protein diffusion through polymer pores and impaired protein interaction with lipophilic molecules [87-88]. The release profile of OVA from these SLNs may be of advantage in the delivery of antigens with the initial fast release facilitating the immune system priming.

5. Conclusions

In this paper, we have demonstrated a microfluidic manufacturing process that is scalable from small laboratory scale to scale-independent processes. Both the total flow rate and the flow rate ratio were identified as critical process parameters and SLNs were produced with particles physicochemical attributes suitable for pre-clinical and potentially clinical application.

6. Acknowledgements

This work was funded by the European Commission Project Leveraging Pharmaceutical Sciences and Structural Biology Training to Develop 21st Century Vaccines (H2020-MSCA-ITN-2015 grant agreement 675370).

7. Supporting information Available

Data presented in this publication can be found at [DOI to be confirmed on acceptance of manuscript].

8. References

[1] Whitesides, G.M., 2006. The origins and the future of microfluidics. Nature 442, 368–373

[2] Bjork S.M. Joensson H.N. Microfluidics for cell factory and bioprocess development. Current Opinion in Biotechnology 2019, 55:95–102

[3] Geoffrey S. The Development of a Low-Cost Microfluidic Magnetic Separation System. 2015-03-13T01:05:59Z

[4] Squires, T.M., Quake, S.R., 2005. Microfluidics: fluid physics at the nanoliter scale. Rev. Modern Phys.(2005) 77, 977

[5] Kastner E., Kaur R.,Lowry D., Moghaddam B., Wilkinson A., Perrie Y. High-throughput manufacturing of size-tuned liposomes by a new microfluidics method using enhanced statistical tools for characterization. International Journal of Pharmaceutics 477 (2014) 361–368

[6] Kastner E., Verma V., Lowry D., Perrie Y. Microfluidic-controlled manufacture of liposomes for the solubilisation of a poorly water soluble drug. International Journal of Pharmaceutics 485 (2015) 122–130

[7] Forbes, N., Hussain, M. T., Briuglia, M. L., Edwards, D. P., ter Horst, J. H., Szita, N., & Perrie Y. Rapid and scale-independent microfluidic manufacture of liposomes entrapping protein incorporating in-line purification and at-line size monitoring. International Journal of Pharmaceutics, (2019) 556, 68-81.

[8] Dimov N., Kastner E., Hussain M., Perrie Y. Szita N. Formation and purification of tailored liposomes for drug delivery using a module-based micro continuous-flow system. Scientific Report, 12045 (2017)

[9] Joshi S., Hussain M.T., Roces C.B., Anderluzzi G., Kastner E., Salmaso S., Kirby D.J., Perrie Y. Microfluidics based manufacture of liposomes simultaneously entrapping hydrophilic and lipophilic drugs. International Journal of Pharmaceutics, (2015) 514 (1). 160–168

[10] Pradhan, P., Guan, J., Lu, D., Wang, P.G., Lee, L.J., Lee, R.J., 2008. A facile microfluidic method for production of liposomes. Anticancer Res. (2008) 28, 943–947.

[11] Pihl J, Karlsson M, Chiu DT. Microfluidic technologies in drug discovery. Drug Discov Today (2005); 10: 1377-83.

[12] Beebe, D. J., Mensing, G. A. & Walker, G. M. Physics and application of microfluidics in biology. Annu. Rev. Biomed. Eng. (2002) 4, 261–286.

[13] Jahn, A., Stavis, S.M., Hong, J.S., Vreeland, W.N., DeVoe, D.L., Gaitan, M. Microfluidic mixing and the formation of nanoscale lipid vesicles. ACS Nano (2010) 4, 2077–2087.

[14] Mazutis L., Vasiliauskas R., Weitz D. A. Microfluidic Production of Alginate Hydrogel Particles for Antibody Encapsulation and Release. Macromol. Biosci.(2015), 15, 1641–1646

[15] Amoyav B., Benny O., Controlled and tunable polymer particles' production using a single microfluidic device. Applied Nanoscience (2018) 8:905–914

[16] C. Zhang, X. Zhang, W. Zhao, C. Zeng, W. Li, B. Li, X. Luo, J. Li, J. Jiang, B. Deng, D.W. McComb, Y. Dong. Chemotherapy drugs derived nanoparticles encapsulating mRNA encoding tumor suppressor proteins to treat triple-negative breast cancer. Nano Res. 2019, 12(4): 855–861

[17] R. Jain, JP. Frederick, EY. Huang, KE. Burke, DM. Mauger, EA. Andrianova, SJ. Farlow, S. Siddiqui, J. Pimentel, K. Cheung-Ong, KM. McKinney, C. Köhrer, MJ. Moore, and T.

Chakraborty. MicroRNAs Enable mRNA Therapeutics to Selectively Program Cancer Cells to Self-Destruct. Nucleic Acid Ther (2018) 28(5):285-296

[18] J. Finn, A. Smith, M. Patel, L. Shaw, M. Youniss, J. Heteren, T. Dirstine, C. Ciullo, R. Lescarbeau, J. Seitzer, R. Shah, A. Shah, D. Ling, J. Growe, M. Pink, E. Rohde, K. Wood, W. Salomon, W. Harrington, C. Dombrowski, W. Strapps, Y. Chang, D. Morrissey. A Single Administration of CRISPR/Cas9 Lipid Nanoparticles Achieves Robust and Persistent In Vivo Genome Editing. Cell Reports (2018) 22, 2227–2235

[19] Carugo D., Bottaro E., Owen J., Stride E., Nastruzzi C. Liposome production by microfluidics: potential and limiting factors. ScientificRepoRts (2016) 6:25876

[20] Sá Correia M.G., Briuglia M.L., Niosi F. Lamprou D.A. Microfluidic manufacturing of phospholipid nanoparticles: Stability, encapsulation efficacy, and drug release. International Journal of Pharmaceutics. (2017) 516 (1-2) 0378-5173.

[21] Ran R., Middelberg A. P. J., Zhao C.X. Microfluidic synthesis of multifunctional liposomes for tumour targeting. ColloidsandSurfacesB:Biointerfaces 148(2016)402–410

[22] Y. Zhang, H. Tan, J.D. Daniels, F. Zandkarimi, H. Liu, L.M. Borwn, K. Uchida, O.A. O'Connor. B.R. Stockwell. Imidazole Ketone Erastin Induces Ferroptosis and Slows Tumor Growth in a Mouse Lymphoma Model. Cell Chemical Biology (2019) 26, 1–11

[23] Thomas A., Garg S.M., De Souza R.A.G., Ouellet E., Tharmarajah G., Reichert D., Ordobadi M., Ip S., Ramsay E.C. Microfluidic Production and Application of Lipid Nanoparticles for Nucleic Acid Transfection. Multiple Myeloma (2018) 978-1-4939-7865-6

[24] M Yu, L Xu, F Tian, Q Su, N Zheng, Y Yang. Rapid transport of deformation-tuned nanoparticles across biological hydrogels and cellular barriers. Nature Communications (2018) 2041-1723

[25] Y Morikawa, T Tagami, A Hoshikawa, T Ozeki. The Use of an Efficient Microfluidic Mixing System for Generating Stabilized Polymeric Nanoparticles for Controlled Drug Release. Biol. Pharm. Bull. 41, 899–907 (2018) 899

[26] Karnik R., Gu F., Basto P., Cannizzaro C., Dean L., Kyei-Manu W., Langer R. Farokhzad O.C. Microfluidic Platform for Controlled Synthesis of Polymeric Nanoparticles . Nano Lett. (2008) 8, 9, 2906-2912

[27] Belliveau, N.M., Huft, J., Lin, P.J., Chen, S., Leung, A.K., Leaver, T.J., Wild, A.W., Lee, J.B., Taylor, R.J., Tam, Y.K., 2012. Microfluidic synthesis of highly potent limit-size lipid nanoparticles for in vivo delivery of siRNA. Mol. Ther. Nucleic Acids. (2012) 10.1038

[28] S. Sieber, P. Grossen, P. Uhl, P. Detampel, W. Mier, D. Witzigmann, J. Huwyler. Zebrafish as a predictive screening model to assess macrophage clearance of liposomes in vivo. Nanomedicine: Nanotechnology, Biology, and Medicine 17 (2019) 82–93

[29] MN Andersen, A Etzerodt, JH Graversen, LC Holthof, SK Moestrup, M Hokland, HJ Møller. STAT3 inhibition specifically in human monocytes and macrophages by CD163-targeted corosolic acid-containing liposomes. Cancer Immunology, Immunotherapy (2019) 68:489–502

[30] Bartheldyová E., Knotigová P.T., Zachová K., Mašek J., Kulich P., Effenberg R., Zyka D., Hubatka F., Kotouček J., Čelechovská H., Héžová R., Tomečková A., Mašková E., Fojtíková M., Macaulay S., Bystrický P., Paulovičová L., Paulovičová E., Drož L., Ledvina M., Raška M.,

420 Turánek J. N-Oxy lipid-based click chemistry for orthogonal coupling of mannan onto
421 nanoliposomes prepared by microfluidic mixing: Synthesis of lipids, characterisation of
422 mannan-coated nanoliposomes and in vitro stimulation of dendritic cells. Carbohydrate
423 Polymers 207 (2019) 521–532

424 [31] Bartheldyová E., Effenberg R., Mašek J., Procházka L., Knötigová P.T., Kulich P., Hubatka
425 F., Velínská K., Zelníčková J., Zouharová D., Fojtíková M., Hrebík D., Plevka P., Mikulík R.,
426 Miller A.D., Macaulay S., Zyka D., Drož L., Raška M., Ledvina M., Turánek J. Hyaluronic acid
427 surface modified liposomes prepared via orthogonal aminoxy coupling: synthesis of nontoxic
428 aminoxylipids based on symmetrically α-branched fatty acids. Bioconjugate Chem. (2018) 29,
429 7, 2343-2356

430 [32] G. Heuck, R. DeSouza, A. Thomas, I. Backstrom, S.M. Garg, E. Ouellet, J. Singh, S. Chang,
431 K. Marshall, P. Johnson, M. DeLeonardis, A. Armstead, G. Tharmarajah, S. Ip, T.J. Leaver, A.W.
432 Wild, R.J. Taylor and E.C. Ramsay. mRNA-Lipid Nanoparticles: A potent tool for manipulating
433 neuronal genes. Vaccines Vaccin (2017) 2041-1723

434 [33] Abstiens K., Goepferich A.M. Microfluidic manufacturing improves polydispersity of
435 multicomponent polymeric nanoparticles. Journal of Drug Delivery Science and Technology
436 49 (2019) 433–439

437 [34] Zhu C., Yang H., Shen L., Zheng Z., Zhao., Li Q., Yu F., Cen L.Microfluidic preparation of
438 PLGA microspheres as cell carriers with sustainable Rapa release. J Biomater Sci Polym Ed.
439 (2019) 0920-5063

[35] Dong YD., Tchung E., Nowell C., Kaga S., Leong N., Mehta D., Kaminskas LM., Boyd BJ. Microfluidic preparation of drug-loaded PEGylated liposomes, and the impact of liposome size on tumour retention and penetration. J Liposome Res. (2019) 0898-2104

[36] Lallana E., Donno R., Magrì D., Barker K., Nazir Z., Treacher K., Lawrence MJ., Ashford M., Tirelli N. Microfluidic-assisted nanoprecipitation of (PEGylated) poly (d,l-lactic acid-co-caprolactone): Effect of macromolecular and microfluidic parameters on particle size and paclitaxel encapsulation. International Journal of Pharmaceutics 548 (2018) 530–539

[37] Capretto L., Mazzitelli S., Nastruzzi C. Design, production and optimization of solid lipid microparticles (SLM) by a coaxial microfluidic device. Journal of Controlled Release 160 (2012) 409–417

[38] Thorsen T., Roberts R.W., Arnold F.H., Quake S.R. Dynamic Pattern Formation in a Vesicle-Generating Microfluidic Device. Phys. Rev. Lett. (2001), 86, 4163.

[39] Lin XZ, Terepka AD, Hong Y (2004) Synthesis of silver nanoparticles in a continuous flow tubular microreactor. Nano Lett (2004) 4(11):2227–2232

[40] van Swaay, D. Microfluidic methods for forming liposomes. Lab Chip (2013) 13, 752–767.

[41] 5) M.D. Joshi, R.H. Müller, Lipid nanoparticles for parenteral delivery of actives,Eur. J. Pharm. Biopharm. 71 (2) (2009) 161–172

[42] S.S. Shidhaye, R. Vaidya, S. Sutar, A. Patwardhan, V.J. Kadam, Solid lipid nanoparticles and nanostructured lipid carriers – innovative generations of solid lipid carriers, Curr. Drug Deliv. 5 (4) (2008) 24–331.

[43] S.A. Wissing, O. Kayser, R.H. Müller, Solid lipid nanoparticles for parenteral drug delivery, Adv. Drug Deliv. Rev. 56 (9) (2004) 1257–1272.

462 [44] H.R. Kim, I.K. Kim, K.H. Bae, S.H. Lee, Y. Lee, T.G. Park, Cationic solid lipid nanoparticles
463 reconstituted from low density lipoprotein components for delivery of siRNA, Mol. Pharm. 5
464 (4) (2008) 622–631.

465 [45] J. Weiss, E.A. Decker, D.J. McClements, K. Kristbergsson, T. Helgason, T. Solid lipid
466 nanoparticles as delivery systems for bioactive food components.Food Biophysics, 3 (2008)
467 1557-1866

468 [46] M.A. Cerqueira, A.C. Pinheiro, H.D. Silva, P.E. Ramos, M.A. Azevedo, M.L. Flores-López,
469 Rivera M.C., Bourbon A.I., Ramos O.L.,A.A. Vicente. Design of bio-nanosystems for oral
470 delivery of functional compounds. Food Engineering Reviews, (2014) 1866-7910

471 [47] Almelda AJ, Souto E. Solid lipid nanoparticles as a drug delivery system for peptides and
472 proteins. Adv. Drug Deliv. Rev. (2007) 59:478–490

473 [48] Stelzner J.J. Behrens M. Behrens S. Mäder K. Squalene containing solid lipid
474 nanoparticles, a promising adjuvant system for yeast vaccines. Vaccine 36 (2018) 2314–2320

475 [49] Olbrich, C., Mueller, R.H., Tabatt, K., Kayser, O., Schulze, C. and Schade, R. Stable
476 biocompatible adjuvants--a new type of adjuvant based on solid lipid nanoparticles: a study
477 on cytotoxicity, compatibility and efficacy in chicken. Altern. Lab. Anim., (2002) 30(4): 443-58

478 [50] G. Chen, S. Zeng, H. Jia, X. He, Y. Fang, Z. Jing. Adjuvant effect enhancement of porcine
479 interleukin-2 packaged into solid lipid nanoparticles Res. Vet. Sci., 96 (2014) 62–68

480 [51] Xie SY, Wang SL, Zhao BK, Han C, Wang M, Zhou WZ. Effect of PLGA as a polymeric
481 emulsifier on preparation of hydrophilic protein-loaded solid lipid nanoparticles. Colloids Surf.
482 B. (2008) 67:199–204

[52] Sjöström B, Bergenståhl B. Preparation of submicron drug particles in lecithin-stabilized o/w emulsions I. Model studies of the precipitation of cholesteryl acetate. Int. J. Pharm. (1992) 88:53–62

[53] Saraf S, Mishra D, Asthana A, Jain R, Singh S, Jain NK. Lipid microparticles for mucosal immunization against hepatitis B. Vaccine. (2006) 24:45–56

[54] Muller RH, Radtke M, Wissing SA. Nanostructured lipid matrices for improved microencapsulation of drugs. Int. J. Pharm. (2002) 242 (1 – 2):121 – 8

[55] Maeki, M., Saito, T., Sato, Y., Yasui, T., Kaji, N., Ishida, A., Tani, H., Baba, Y., Harashima, H., Tokeshi, M. A strategy for synthesis of lipid nanoparticles using microfluidic devices with a mixer structure. RSC Adv. (2015) 5, 46181–46185.

[56] Patra, M., Salonen, E., Terama, E., Vattulainen, I., Faller, R., Lee, B.W., Holopainen, J., Karttunen, M. Under the influence of alcohol: the effect of ethanol and methanol on lipid bilayers. Biophys. J. (2006) 90, 1121–1135.

[57] Jahn, A., Stavis, S.M., Hong, J.S., Vreeland, W.N., DeVoe, D.L., Gaitan, M. Microfluidic mixing and the formation of nanoscale lipid vesicles. ACS Nano (2010) 4, 2077–2087.

[58] 26) Zhigaltsev, I.V., Belliveau, N., Hafez, I., Leung, A.K., Huft, J., Hansen, C., Cullis, .R.P. Bottom-up design and synthesis of limit size lipid nanoparticle systems with aqueous and triglyceride cores using millisecond microfluidic mixing. Langmuir (2012) 28, 3633–3640

[59] Zook, J.M., Vreeland, W.N. Effects of temperature, acyl chain length, and Flow rate ratio on liposome formation and size in a microfluidic hydrodynamic focusing device. Soft Matter (2010) 6, 1352–1360.

504 [60] Balbino, T.A., Azzoni, A.R., de La Torre, L.G. Microfluidic devices for continuous
505 production of pDNA/cationic liposome complexes for gene delivery and vaccine therapy.
506 Colloid Surf. B (2013) 111, 203–210

507 [61] Mehnert W, Mader K. Solid Lipid Nanoparticles - Production, Characterization and
508 Applications. Adv Drug Delivery Rev. (2001) 47:165–196.

509 [62] Xue HY, Wong HL. Tailoring Nanostructured Solid-Lipid Carriers for Time-Controlled
510 Intracellular siRNA Kinetics to Sustain RNAi-Mediated Chemosensitizationd. Biomaterials.
511 (2011) 32:2662–2672.

512 [63] Wissing SA, Kayser O, Muller RH. Solid Lipid Nanoparticles for Parenteral Drug Delivery.
513 Advanced Drug Delivery Reviews. (2004) 56:1257–1272.

514 [64] Wang R., Xiao R., Zeng Z.,Xu L., Wang J. Application of poly(ethylene glycol)–
515 distearoylphosphatidylethanolamine (PEG-DSPE) block copolymers and their derivatives as
516 nanomaterials in drug delivery. Int J Nanomedicine. (2012) 7: 4185–4198.

517 [65] Wu H.,Zhu L.,Torchilin V.P. pH-sensitive poly(histidine)-PEG/DSPE-PEG co-polymer
518 micelles for cytosolic drug delivery. Biomaterials. (2013) 34(4): 1213–1222.

519 [66] Lobovkina, T., Jacobson, G. B., Gonzalez-Gonzalez, E., Hickerson, R. P., Leake, D., Kaspar,
520 R. L., H. Contag C.H., Zare, R. N. In vivo sustained release of siRNA from solid lipid
521 nanoparticles. ACS nano. (2011) 5(12), 9977–9983.

522 [67] Uner, M., & Yener, G. Importance of solid lipid nanoparticles (SLN) in various
523 administration routes and future perspectives. International journal of nanomedicine. (2007)
524 2(3), 289–300.

525 [68] Kashanian S. Rostami E. PEG-stearate coated solid lipid nanoparticles as levothyroxine
526 carriers for oral administration. J Nanopart Res (2014) 16:2293

527 [69] Bahl, K., Senn, J.J., Yuzhakov, O., Bulychev, A., Brito, L.A., Hassett, K.J., Laska, M.E., Smith,
528 M., Almarsson, Ö., Thompson, J., et al. (2017). Preclinical and clinical demonstration of
529 immunogenicity by mRNA vaccines against H10N8 and H7N9 influenza viruses. Mol.
530 Ther.(2017) 25, 1316–1327.

531 [70] Lam Y, Gan H, Nguyen N, Lie H. Micromixer based on viscoelastic flow instability at low
532 Reynolds number. Biomicrofluid. (2009) 3:014106

533 [71] Huang MZ, Yang RJ, Tai CH, Tsai CH, Fu LM. Application of electrokinetic instability flow
534 for enhanced micromixing in cross-shaped microchannel. Biomed. Microdevices. (2006)
535 8:309–315

536 [72] Meijer HEH, Singh MK, Kang TG, den Toonder JMJ, Anderson PD. Passive and active
537 mixing in microfluidic devices. Macromol. Symp. (2009)279:201–209.

538 [73] ICH. Harmonized tripartite guideline, Q3C impurities: residual solvents. Fed Reg
539 (1997)62:67377.

540 [74] Klok R.P., Windhorst A.D. Residual solvent analysis by gas chromatography in
541 radiopharmaceutical formulations containing up to 12% ethanol. Nuclear Medicine and
542 Biology 33 (2006) 935–938

543 [75] Qin L, Hu CQ, Yin LH. Establishment of a knowledge base for prescreening residual
544 solvents in pharmaceuticals. Chromatographia (2004) 59:475–80.

545 [76] Schwartz L. Desalting and Buffer Exchange by Dialysis, Gel Filtration, or Diafiltration. Pall
546 Life Sciences.

547 [77] Schwartz L., Seeley K. Introduction to Tangential Flow Filtration for Laboratory and
548 Process Development Applications. Pall Life Sciences

549 [78] Dalwadi G., Sunderland V. Purification of PEGylated Nanoparticles Using Tangential Flow
550 Filtration (TFF). Drug Development and Industrial Pharmacy,(2007) 33:9, 1030-1039.

551 [79] Hirsjärvi S., Peltonen L.,Hirvonen J. Effect of Sugars, Surfactant, and Tangential Flow
552 Filtration on the Freeze-Drying of Poly(lactic acid) Nanoparticles. AAPS PharmSciTech. (2009)
553 10(2): 488–494.

554 [80] S. Morel, E. Ugazio, R. Cavalli, M.R. Gasco, Thymopentin in solid lipid nanoparticles, Int.
555 J. Pharm. 132 (1996) 259–261

556 [81] E. Ugazio, R. Cavalli,M.R. Gasco, Incorporation of cyclosporine A in solid lipid
557 nanoparticles (SLN), Int. J. Pharm. 241 (2002) 341–344

558 [82] Salmaso, Bersani S., Elvassore N., Bertucco A., Caliceti P. Biopharmaceutical
559 characterisation of insulin and recombinant human growth hormone loaded lipid submicron
560 particles produced by supercritical gas micro-atomisation. International Journal of
561 Pharmaceutics 379 (2009) 51–58

562 [83] Salmaso, Elvassore N., Bertucco A., Caliceti P Production of solid lipid submicron particles
563 for protein delivery using a novel supercritical gas-assisted melting atomization process.
564 Journal of Pharmaceutical Sciences. 10 (2009) 1002

565 [84] Jahn, A., Reiner, J., Vreeland, W., DeVoe, D., Locascio, L., Gaitan, M. Unexpectedly high
566 entrapment efficiencies in nanometer scale liposomes with hydrodynamic focusing using
567 continuous-flow microfluidics. Twelfth International Conference on Miniaturized Systems for
568 Chemistry and Life Sciences. (2008) 978-0-9798064

569 [85] A. Jahn, W.N. Vreeland, D.L. DeVoe, L.E. Locascio, M. Gaitan., Microfluidic directed
570 formation of liposomes of controlled size, Langmuir, (2007) 23 (11), 6289-6293.

571 [86] Wilson B., Samanta M.K., Santhi K., Kumar K.P.S., Paramakrishnan N., Suresh B.; Poly(n-
572 butylcyanoacrylate) nanoparticles cated with polysorbate 80 for the targeted delivery of
573 rivastigmine into the brain to treat Alzheimer's disease. Brain Research, (2008)

574 [87] Liu J, Gong T, Wang C, Zhong Z, Zhang Z. Solid lipid nanoparticles loaded with insulin by
575 sodium cholate-phosphatidylcholine-based mixed micelles: preparation and characterization.
576 Int. J. Pharm. (2007) 340:153–162

577 [88] Zhang X.,Chen G.,Zhang T., Ma Z., Wu B. Effects of PEGylated lipid nanoparticles on the
578 oral absorption of one BCS II drug: a mechanistic investigation. Int J Nanomedicine. (2014) 9:
579 5503–5514.

580

581 **Tables.**

582 **Table 1.** Examples of research investigating the use of microfluidics technology for the
583 manufacture of nanoparticles.

Title	Application	Year	Ref
Microfluidic Production of Alginate Hydrogel Particles for Antibody Encapsulation and Release	Alginate Hydrogel Particles	2015	14
Controlled and tunable polymer particles' production using a single microfluidic device	Polymeric nanoparticles	2018	15
Chemotherapy drugs derived nanoparticles encapsulating mRNA encoding tumor suppressor proteins to treat triple-negative breast cancer	Lipid nanoparticle	2019	16
MicroRNAs Enable mRNA Therapeutics to Selectively Program Cancer Cells to Self-Destruct	Lipid nanoparticle	2018	17
A Single Administration of CRISPR/Cas9 Lipid Nanoparticles Achieves Robust and Persistent In Vivo Genome Editing	Lipid nanoparticles	2018	18
High-throughput manufacturing of size-tuned liposomes by a new microfluidics method using enhanced statistical tools for characterization	Liposomes	2014	5
Microfluidic-controlled manufacture of liposomes for the solubilisation of a poorly water soluble drug	Liposomes	2015	6
Rapid and scale-independent microfluidic manufacture of liposomes entrapping protein incorporating in-line purification and at-line size monitoring	Liposomes	2019	7
Formation and purification of tailored liposomes for drug delivery using a module-based micro continuous-flow system	Liposomes	2017	8
Microfluidics based manufacture of liposomes simultaneously entrapping hydrophilic and lipophilic drugs	Liposomes	2016	9
Liposome production by microfluidics: potential and limiting factors	Liposomes	2016	19
Microfluidic manufacturing of phospholipid nanoparticles: Stability, encapsulation efficacy, and drug release	Liposomes	2016	20
Microfluidic synthesis of multifunctional liposomes for tumour targeting	Liposomes	2016	21
Imidazole Ketone Erastin Induces Ferroptosis and Slows Tumor Growth in a Mouse Lymphoma Model	Polymeric nanoparticles	2019	22
Microfluidic Production and Application of Lipid Nanoparticles for Nucleic Acid Transfection	Lipid nanoparticles	2018	23
Rapid transport of deformation-tuned nanoparticles across biological hydrogels and cellular barriers	Polymeric nanoparticles	2018	24

The Use of an Efficient Microfluidic Mixing System for Generating Stabilized Polymeric Nanoparticles for Controlled Drug Release	Polymeric nanoparticles	2018	25
Microfluidic Platform for Controlled Synthesis of Polymeric Nanoparticles	Polymeric nanoparticles	2008	26
Microfluidic synthesis of highly potent limit-size lipid nanoparticles for in vivo delivery of siRNA.	Lipid nanoparticles	2012	27
Zebrafish as a predictive screening model to assess macrophage clearance of liposomes in vivo	Liposomes	2019	28
STAT3 inhibition specifically in human monocytes and macrophages by CD163-targeted corosolic acid-containing liposomes	Liposomes	2019	29
N-Oxy lipid-based click chemistry for orthogonal coupling of mannan onto nanoliposomes prepared by microfluidic mixing: Synthesis of lipids, characterisation of mannan-coated nanoliposomes and in vitro stimulation of dendritic cells	Liposomes	2018	30
Hyaluronic acid surface modified liposomes prepared via orthogonal aminoxy coupling: synthesis of nontoxic aminoxylipids based on symmetrically α-branched fatty acids	Liposomes	2018	31
mRNA-Lipid Nanoparticles: A potent tool for manipulating neuronal genes	Lipid nanoparticles	2017	32
Microfluidic manufacturing improves polydispersity of multicomponent polymeric nanoparticles	Polymeric nanoparticles	2019	33
Microfluidic preparation of PLGA microspheres as cell carriers with sustainable Rapa release	Polymeric nanoparticles	2019	34
Microfluidic preparation of drug-loaded PEGylated liposomes, and the impact of liposome size on tumour retention and penetration	Liposomes	2019	35
Microfluidic-assisted nanoprecipitation of (PEGylated) poly (d,l-lactic acid-co-caprolactone): Effect of macromolecular and microfluidic parameters on particle size and paclitaxel encapsulation	Polymeric nanoparticles	2018	36
Design, production and optimization of solid lipid microparticles (SLM) by a coaxial microfluidic device	Solid lipid microparticles	2012	37
Dynamic Pattern Formation in a Vesicle-Generating Microfluidic Device	reverse micelles	2001	38
Synthesis of silver nanoparticles in a continuous flow tubular microreactor	Silver nanoparticles	2004	39

584

585

Figure legends

Figure 1. Microfluidic and solid lipid nanoparticles publications in engineering, multidisciplinary, and biology and medicine journals from 1980 to 2019.

Figure 2. A) Size (columns) and PDI (dots) and B) Intensity plot of SLNs made by Nanoassemblr and sized after dialysis purification method. FRR 1:1 (black solid line), 3:1 (black dashed line) and 5:1(gray solid line) were represented and C) Zeta-potential of Tristearin: mPEG-DSPE SLNs using Nanoassemblr after dialysis. Formulations with TFR 10 mL/min and FRR from 1:1 to 5:1 had been tested. Results are expressed as the means of three experiments ± S.D.

Figure 3. Purification of SLNs. Formulations were prepared using a TFR of 10 mL/min and FRR of 1:1. A) Lipid recovery of Tristearin: mPEG-DSPE SLNs after spin column, dialysis and TFF purification and B) Residual solvent after spin column, dialysis and TFF expressed as percentage of remained ethanol (mL%). All data were normalised by IPA standard peaks area. Results are expressed as the means of three experiments ± S.D.

Figure 4. The effect of digestion method on entrapment. Solid lipid nanoparticles encapsulating 0.1, 0.5 and 1 mg/mL initial OVA content were formulated using the Nanoassemblr platform. A) Protein encapsulation efficiency was determined after 3 min, 6 hours and 24 hours post IPA digestion. Protein incorporation also expressed as B) Protein loading efficiency (%) and C) Loading capacity (wt OVA/wt Tristearin). Results are expressed as the means of at least four experiments ± SD.

Figure 5. A) Size (columns), PDI (dots), B) Zeta potential and C) Loading capacity (µg/mL) of OVA loaded SLNs. Initial protein concentration was 0.5 mg/mL. FRR was set up at 3:1 while TFR were increased between 5 and 20 mL/min. Results are expressed as the means of at least four experiments ± SD.

Figure 6. A) The cumulative release profile of OVA under physiological conditions from SLNs (PBS buffer, pH = 7.4, at 37°C). B) Data was also replotted according to first-order models. Results represent percentage cumulative release of initially incorporated OVA and are expressed as the means of three experiments ±SD.

Tristearin &
1,2-Distearoyl-
phosphatidylethanolamine-mPEG2000

Protein in buffer pH 7.4

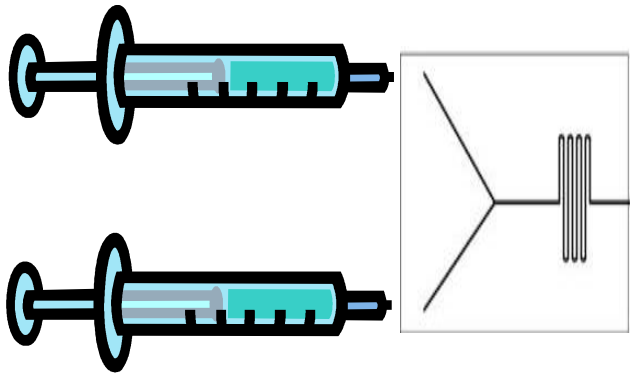

Solid lipid
nanoparticles

Checklist of CPPs

- ✓ Protein concentration
- ✓ Flow rate ratio
- ✓ Total flow rate

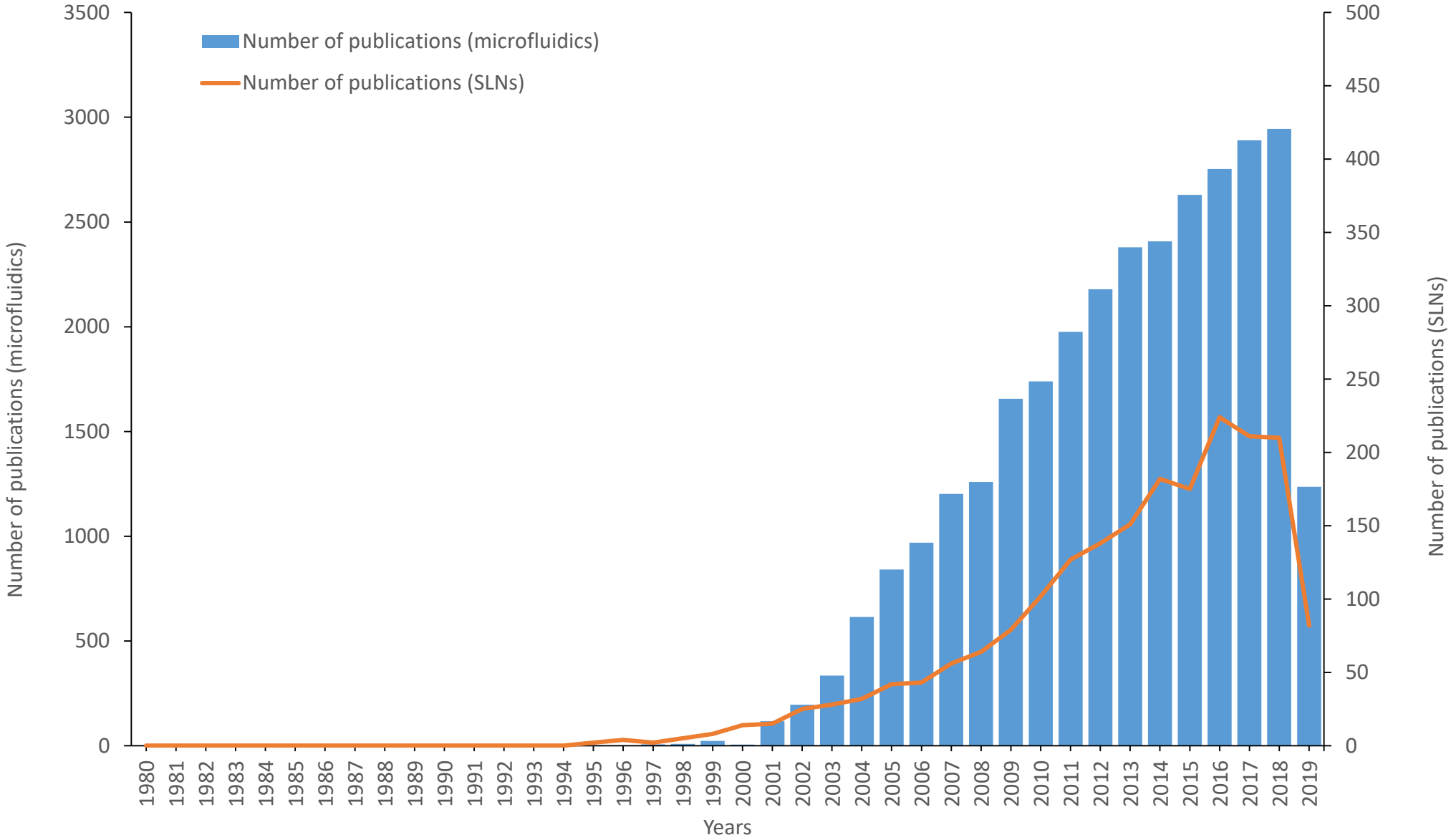
Number of publications (microfluidics)
Number of publications (SLNs)
Number of publications (microfluidics)
Number of publications (SLNs)
Years
3500
3000
2500
2000
1500
1000
500
0
500
450
400
350
300
250
200
150
100
50
0
1980
1981
1982
1983
1984
1985
1986
1987
1988
1989
1990
1991
1992
1993
1994
1995
1996
1997
1998
1999
2000
2001
2002
2003
2004
2005
2006
2007
2008
2009
2010
2011
2012
2013
2014
2015
2016
2017
2018
2019

Figure 1

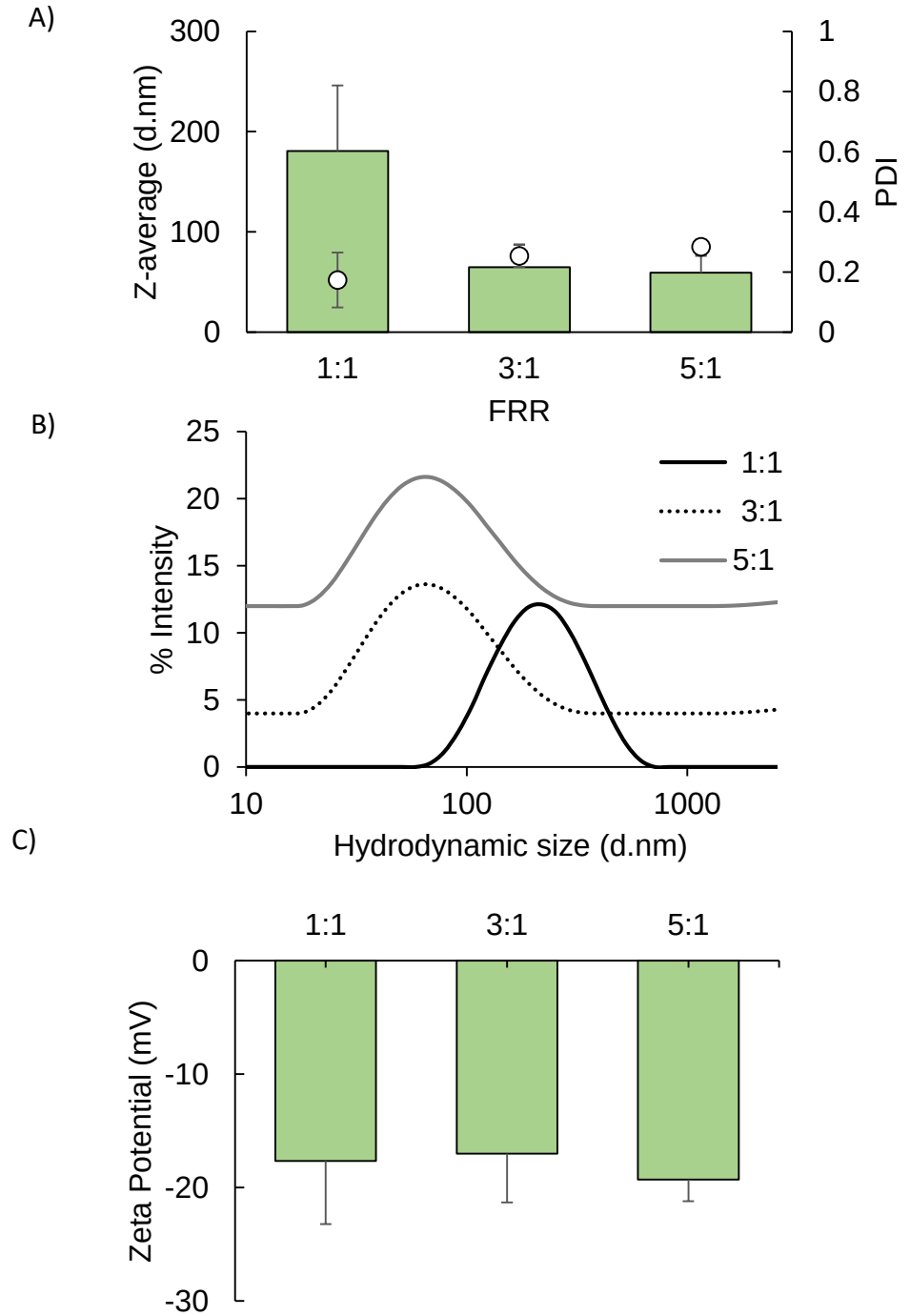
A)
300
200
100
0
Z-average (d.nm)
1
0.8
0.6
0.4
0.2
0
PDI
1:1
3:1
5:1
FRR
B)
25
20
15
10
5
0
% Intensity
1:1
3:1
5:1
10
100
1000
Hydrodynamic size (d.nm)
C)
1:1
3:1
5:1
0
-10
-20
-30
Zeta Potential (mV)

Figure 2

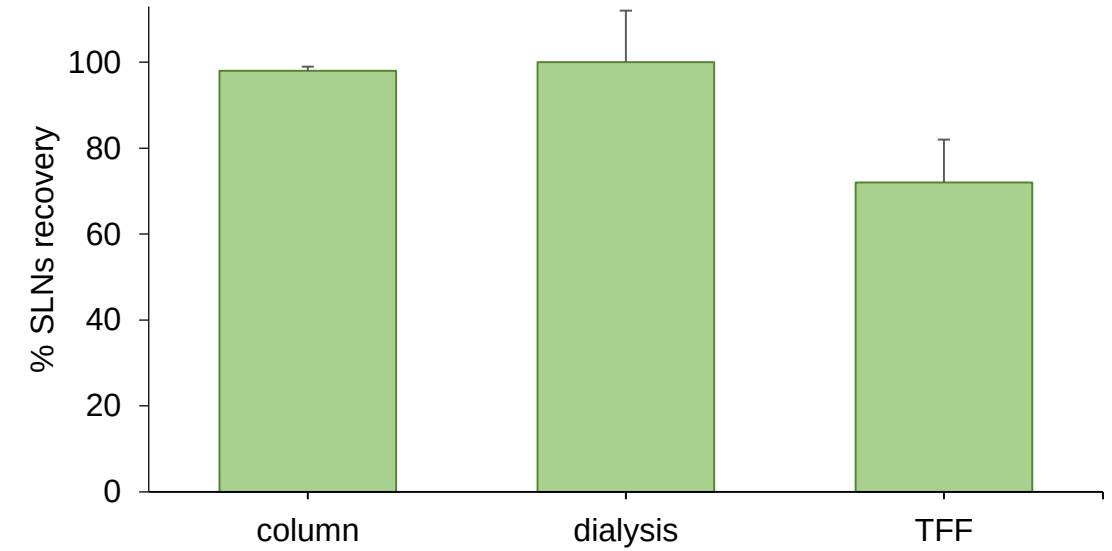
% SLNs recovery
100
80
60
40
20
0
column
dialysis
TFF

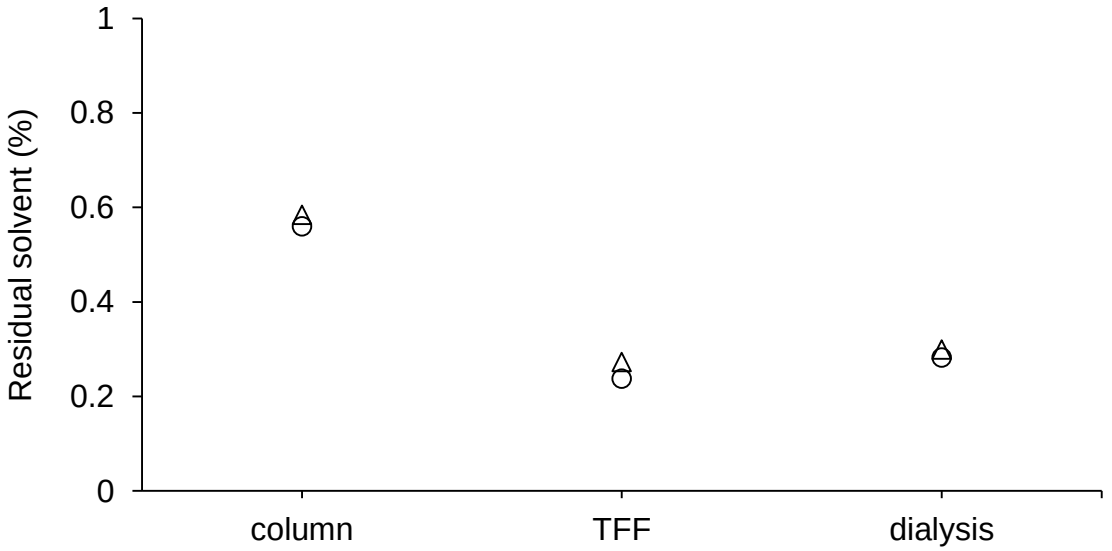
Residual solvent (%)
1
0.8
0.6
0.4
0.2
0
column
TFF
dialysis

Figure 3

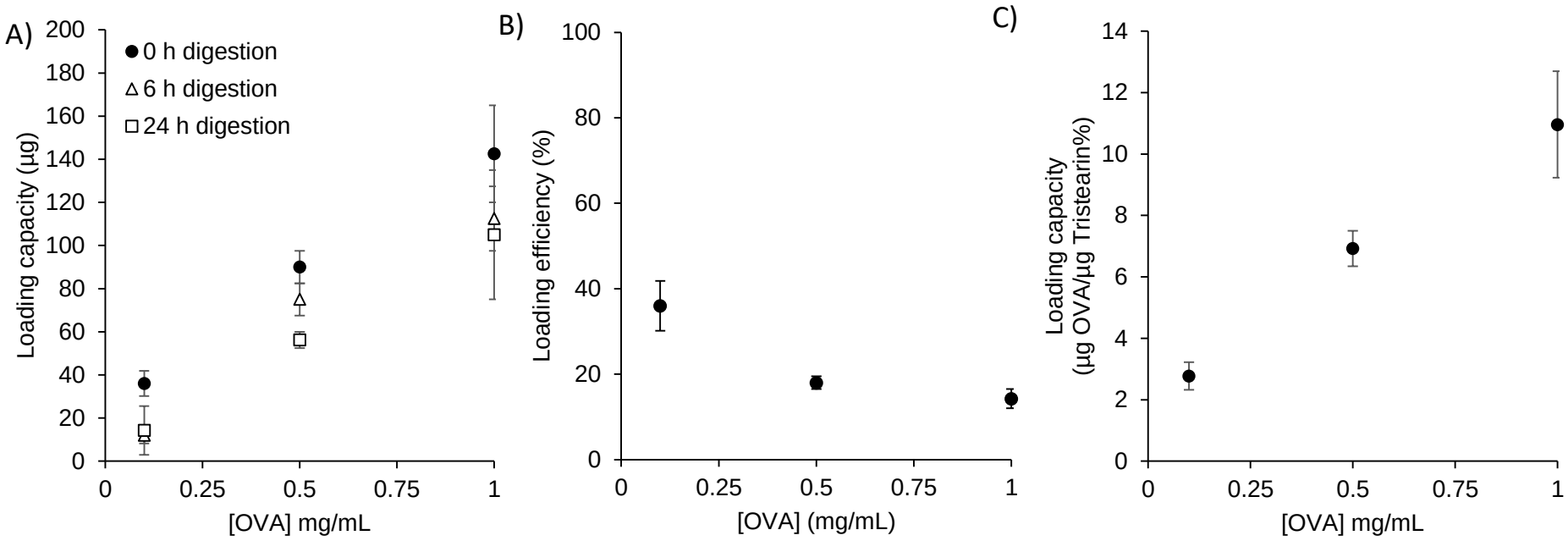
A)
0 h digestion
6 h digestion
24 h digestion
Loading capacity (µg)
[OVA] mg/mL
B)
Loading efficiency (%)
[OVA] (mg/mL)
C)
Loading capacity
(µg OVA/µg Tristearin%)
[OVA] mg/mL

Figure 4

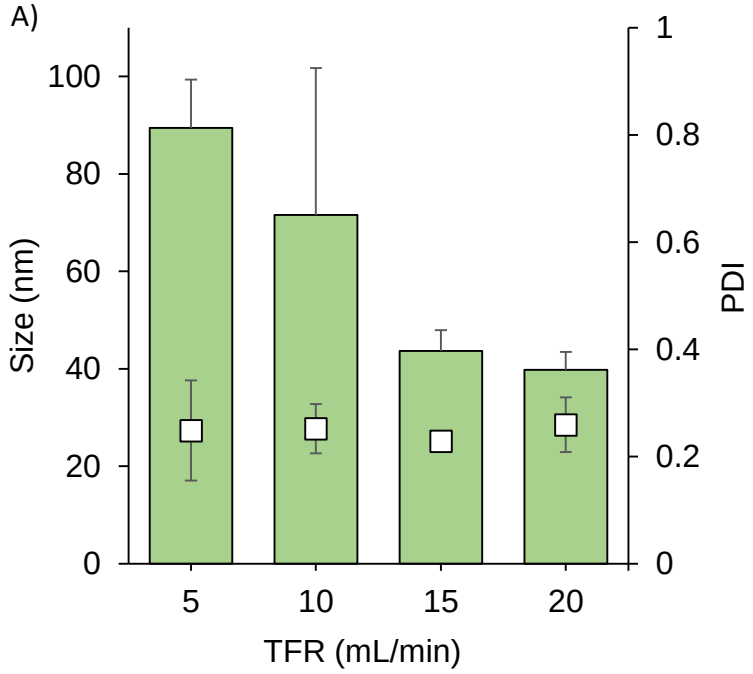
A)
Size (nm)
PDI
TFR (mL/min)
0
20
40
60
80
100
0
0.2
0.4
0.6
0.8
1
5
10
15
20

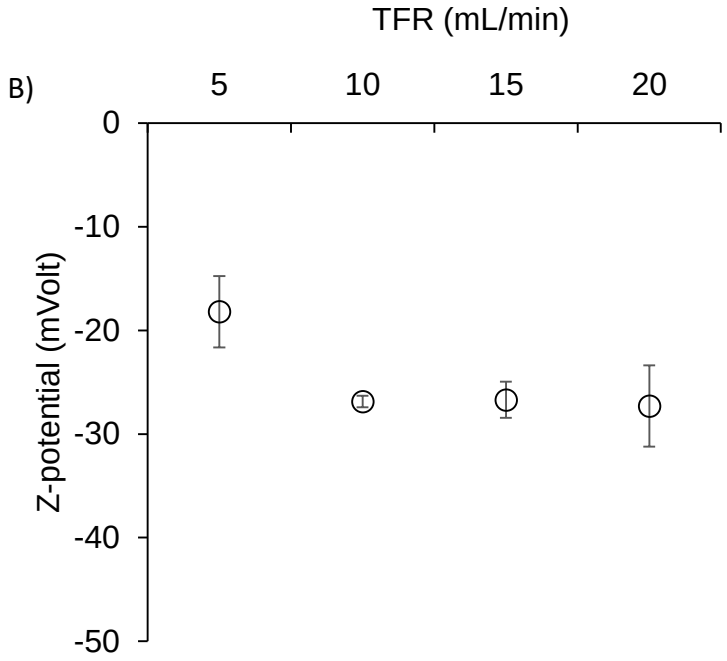
B)
TFR (mL/min)
Z-potential (mVolt)
5
10
15
20
0
-10
-20
-30
-40
-50

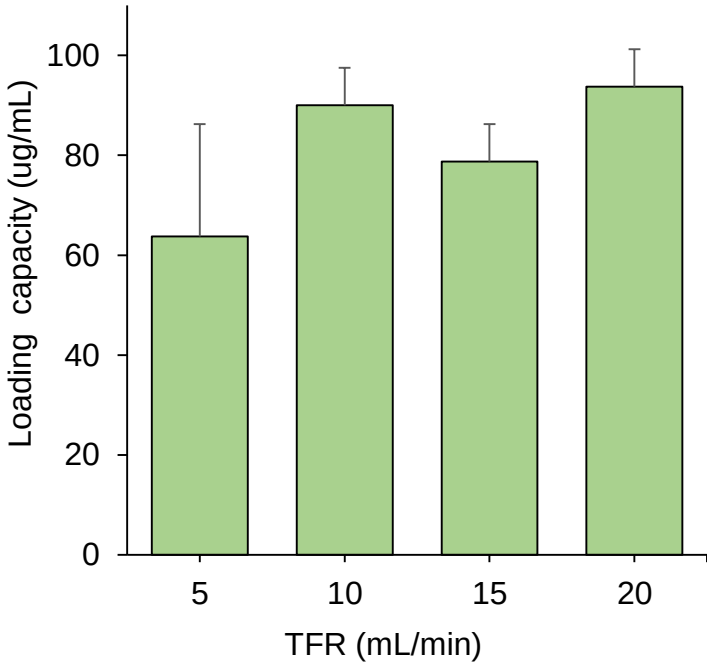
C)
Loading capacity (ug/mL)
TFR (mL/min)
0
20
40
60
80
100
5
10
15
20

Figure 5

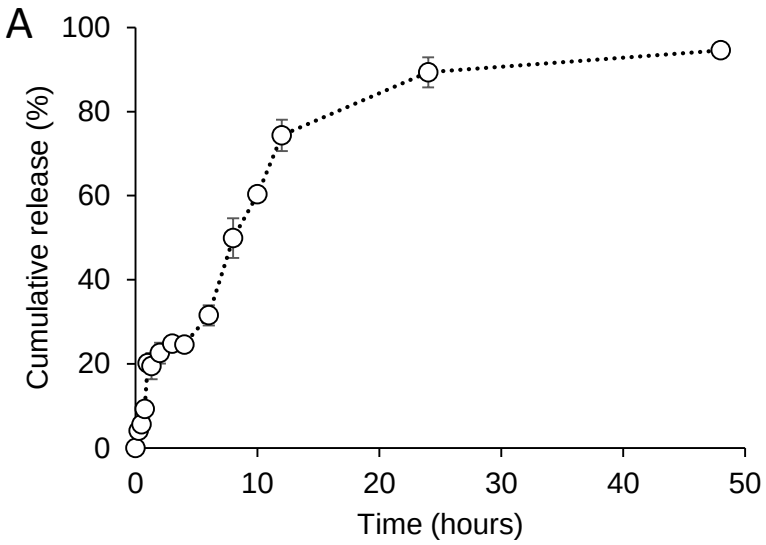
A
100
80
60
40
20
0
Cumulative release (%)
0
10
20
30
40
50
Time (hours)

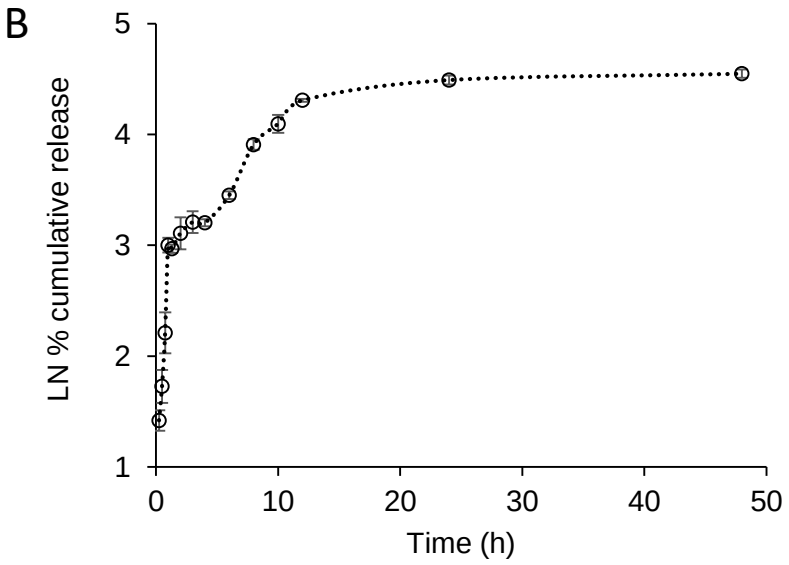
B
5
4
3
2
1
LN % cumulative release
0
10
20
30
40
50
Time (h)